JOURNAL OF AIRCRAFT
Vol. 46, No. 5, September–October 2009

Flying Qualities for a Twin-Jet Transport in Severe Atmospheric Turbulence

Ray C. Chang* and Cun-En Ye†
China Institute of Technology, Hsin-Chu 312, Taiwan, Republic of China
C. Edward Lan‡
University of Kansas, Lawrence, Kansas 66045
and
Michael Guan§
Aviation Safety Council, Taipei County 231, Taiwan, Republic of China

DOI: 10.2514/1.42408

Atmospheric turbulence is the leading cause of serious personal injuries in nonfatal accidents of commercial aircraft. One main type of motion that causes flight injuries in atmospheric turbulence is the sudden plunging motion with an abrupt change in altitude. To assess the possibility of designing a control system to mitigate such plunging motion, the dynamic stability characteristics must be known. The main objective of the present paper is to evaluate the dynamic stability characteristics and, more generally, the flying qualities of a twin-jet transport aircraft encountering severe atmospheric turbulence through digital six-degree-of-freedom flight simulations in transonic flight. The fuzzy-logic thrust model and unsteady aerodynamic models are used to estimate the nonlinear unsteady aerodynamics while performing numerical integration of flight dynamic equations. The flying qualities are based on the instantaneous eigenvalues of all flight modes obtained during time integration. It is shown that the real part of eigenvalues for the plunging mode (i.e., damping characteristics) is largely positive and can be used as a key parameter in describing the flying qualities in plunging.

Nomenclature

a_n	=	normal accelerations, g
b	=	wing span, m
C_x, C_z, C_m	=	longitudinal aerodynamic force and moment coefficients
C_y, C_l, C_n	=	lateral-directional aerodynamic force and moment coefficients
$\bar{c}$	=	mean aerodynamic chord, m
h	=	altitude, m
I_{xx}, I_{yy}, I_{zz}	=	moments of inertia about the x, y, and z axes, $\text{kg} \cdot \text{m}^2$
I_{xy}, I_{xz}, I_{yz}	=	products of inertia, $\text{kg} \cdot \text{m}^2$
k_1, k_2	=	longitudinal and lateral-directional reduced frequencies
L, M, N	=	moments acting along the (x, y, z)-body axes of the aircraft, $\text{N} \cdot \text{m}$
L/D	=	lift-to-drag ratio
M	=	Mach number
m	=	aircraft mass, kg
$\dot{m}_f$	=	fuel flow rate, kg/hr
N_1	=	the rpm of the compressor, rpm
p, q, r	=	body axis roll rate, pitch rate, and yaw rate, deg./s
$\bar{q}$	=	dynamic pressure, kpa
S	=	wing reference area, m^2
T, W	=	thrust and aircraft weight in flight, N
T/W	=	thrust-to-weight ratio
T_2	=	time to double or halve the amplitude, s
t	=	time, s
X, Y, Z	=	forces acting on the aircraft body-fixed axes about the x, y, and z axes, N
α, $\dot{\alpha}$	=	angle of attack, deg and time rate of angle of attack, deg/s
α_m, α_g	=	angles of attack due to motion only and the total angle of attack, deg
β, $\dot{\beta}$	=	sideslip angle, deg and time rate of sideslip angle, deg/s
γ	=	climb angle, deg
δ_a, δ_e, δ_r	=	control deflection angles of aileron, elevator and rudder, deg
ζ	=	damping ratio
λ_r, λ_i	=	eigenvalue in real (i.e., in phase) and imaginary (i.e., out-of-phase) parts
ϕ, θ, ψ	=	Euler angles in roll, pitch, and yaw, deg
ω_n	=	natural frequency

Received 26 November 2008; revision received 15 March 2009; accepted for publication 17 March 2009.

*Associate Professor, Aviation Mechanical Engineering Department; raychang@cc.hc.chit.edu.tw.
†Research Assistant, Aviation Mechanical Engineering Department; yn_0_0@hotmail.com.
‡J.L. Constant Distinguished Professor Emeritus, Aerospace Engineering Department; vortex@ku.edu. Associate Fellow AIAA.
§Director, Investigation Laboratory; michael@asc.gov.tw.

I. Introduction

ONE of the objectives in NASA's flight safety program, which was initiated in 1997, has been establishing hazard indices for flight in atmospheric turbulence. So far, the proposed hazard index has been all related to structural loads. In [1], the turbulence hazard is quantified in terms of the root-mean-square (rms) normal loads over a moving 5 s interval to define the severity of turbulence. The correlation coefficient of the rms normal loads to the peak loads is determined to be 0.89 in 102 cases. The estimation was based on the assumption of continuous turbulence. However, experience indicates that most flight injuries in atmospheric turbulence have been caused by sudden plunging motion with a localized region of strong turbulence.

To predict the hazard levels for any aircraft, the effects of altitude, aircraft type, weight, airspeed, etc., must be considered. Therefore, flight dynamic equations should be employed. There have been

several studies in this regard in the literature. For example, in [2], the atmospheric turbulence severity was estimated in real time from in situ aircraft measurements. The purpose was to calculate the eddy dissipation rate from the measurement of the aircraft normal acceleration based on the assumption of a homogeneous, continuous, linear von Kármán turbulence model coupled with a linear transfer function of the aircraft dynamics. This model of the National Center of Atmospheric Research is intended for continuous-turbulence environments. Another approach of a normal-force in situ turbulence algorithm for aircraft [3] was toward skipping the measure of turbulence itself (i.e., eddy dissipation rate) and directly reporting (or deriving) the aircraft response (hazard) instead, still based on steady linear aerodynamics. Similarly, Buck et al. [4] calculated the distributed loads across the cabin based on small perturbations about the trim in pitch-plunge motions. An issue here is whether peak loads can represent the characteristics of stability and controllability of an airplane is uncertain. Stability and controllability are certainly the focus of flight safety.

In reality, an airplane's aerodynamics and flight characteristics can vary rapidly when subject to atmospheric turbulence. These fast-varying characteristics not only pose threats to flight safety, but also may cause structural damages and reduce fatigue life. To effectively analyze the performance degradation, structural response, and variations in stability and controllability of the aircraft encountering turbulence, the nonlinear unsteady aerodynamic models would be needed [5,6]. In all existing simulations, the imposed external wind field may be turbulent, but the response aerodynamics has been mostly steady. This may explain why stability and control analysis of an airplane in severe atmospheric turbulence has been scarce.

In this paper, a modeling method based on a fuzzy-logic algorithm to estimate unsteady aerodynamic models [7,8], including thrust models, for a twin-jet transport by using the data from the quick-access recorder (QAR) and flight manual will be presented. Flying qualities are used to define how well an airplane can be flown to achieve the mission requirements with flight safety assurance and are described by the interaction between the control inputs and airplane response within the operational flight envelope. Of course, the magnitude of control forces and the control gradients are relevant, as they affect the pilot ratings. For airplanes with irreversible control systems, the flying qualities related to the control forces cannot be evaluated by the present approach and therefore will not be considered further. Specifically, the instantaneous eigenvalues of all flight modes will be evaluated while time integration of flight dynamic equations incorporating with realistic dynamic aerodynamics is performed.

II. Theoretical Development

The present approach is to evaluate the dynamic stability characteristics and flying qualities while integrating the flight dynamics equations of motion. In a numerical flight simulation, models in thrust, aerodynamics, and moments of inertia are needed. For the moments of inertia, fuzzy-logic models based on dimensionless radii of gyration for some existing transport airplanes [9] are developed for interpolation and extrapolation. The parameters in the models are weight, span, overall airplane length, and the number of engines. Although the models are somewhat rough, they are consistent with those used in setting up the aerodynamic models. Establishments of thrust and aerodynamic models, as well as numerical simulation, are described in the following.

A. Fuzzy-Logic Thrust Model

In general, the thrust terms may appear in the equations of motion as three-axis forces and moments. For a transport airplane, only the axial force and the pitching moment are assumed to be affected by thrust. However, the effect of severe clear-air turbulence on the engine parameters and the thrust magnitude are not known and are therefore ignored.

In developing a fuzzy-logic thrust model, data from the flight manual for the fuel flow rates $\dot{m}_f$ at various altitudes h, weights W, Mach numbers M, calibrated airspeed (CAS), and engine pressure ratios (EPRs) in cruise flight are used. The corresponding magnitude of thrust is calculated by assuming a lift-to-drag ratio L/D of 17.5. This value of lift to drag in cruise is assumed based on the past design experience for twin-jet transports [10]. Additional data are supplemented from the QAR data in the climbing and descending phases in which the climb or descent rates are known. For the Pratt & Whitney engines, thrust T is defined by EPR, and so the thrust model is set up as

$$T = f(h, W, M, \text{CAS}, \text{EPR}, \dot{m}_f) \tag{1}$$

For General Electric Company engines, the rpm of the low-pressure compressor N_1 is used to set the level of thrust, and so the thrust model is set up as

$$T = f(h, W, M, \text{CAS}, N_1, \dot{m}_f) \tag{2}$$

In the present study, the Pratt & Whitney engines powering one twin-jet transport will be illustrated.

The QAR data in climb and descent are also used, in addition to the cruise data, in thrust model development. The following climb equations are to be satisfied in the least-squares sense over a 5 s interval:

$$\frac{W}{g}\frac{dV}{dt} = T - D - W\sin\gamma \tag{3}$$

and

$$\frac{D}{W} = \frac{D}{L}\cos\gamma \tag{4}$$

All these equations are still valid in descent with negative climb angles γ. Thrust is estimated from the preceding equations with the drag- and lift-coefficient models preestimated from the same set of data in cruise at a lower Mach number.

Once the thrust model is generated as a function of h, W, M, CAS, EPR, and $\dot{m}_f$ with the flight conditions of climbing, cruise, and descent, we can estimate the thrust magnitude by inserting these flight variables from the QAR into the model.

B. Fuzzy-Logic Unsteady Aerodynamic Model

In this model, more complete influencing flight variables can be included to capture all possible effects on an aircraft encountering hazardous weather. For longitudinal aerodynamics, these variables include [7,8]

$$C_x, C_z, C_m = f(\alpha, \dot{\alpha}, q, k_1, \beta, \delta_e, M, p, \delta_s, \bar{q}) \tag{5}$$

The coefficients on the left-hand side of Eq. (5) represent the coefficients of axial force C_x, normal force C_z, and pitching moment C_m. The variables on the right-hand side of Eq. (5) denote the angle of attack α, time rate of angle of attack $d\alpha/dt$ or $\dot{\alpha}$, pitch rate q, longitudinal reduced frequency k_1, sideslip angle β, control deflection angle of elevator δ_e, Mach number M, roll rate p, stabilizer angle δ_s, and dynamic pressure $\bar{q}$. These variables are called the influencing variables. The roll rate is included here because it is known that an aircraft encountering hazardous weather tends to develop rolling that may affect longitudinal stability. The inclusion of dynamic pressure is for estimation of the significance in structural deformation effects.

For the lateral-directional aerodynamics [7,8],

$$C_y, C_l, C_n = f(\alpha, \beta, \phi, p, r, k_2, \delta_a, \delta_r, M, \dot{\alpha}, \dot{\beta}) \tag{6}$$

The coefficients on the left-hand side of Eq. (6) represent the coefficients of side force C_y, rolling moment C_l, and yawing moment C_n. The variables on the right-hand side of Eq. (6) denote the angle of attack α, sideslip angle β, roll angle ϕ, roll rate p, yaw rate r, lateral-directional reduced frequency k_2, control deflection angle of aileron δ_a, control deflection angle of rudder δ_r, Mach number M, time rate of angle of attack $\dot{\alpha}$, and time rate of sideslip angle $\dot{\beta}$.

C. Flight Simulation

In civil airplane design, there are no numerical guidelines for flying quality. On the other hand, the guidelines are expressed in damping ratios and natural frequencies and the time to double or halve the amplitude of initial disturbances in the military airplane design, which are described in [11]. The latter is defined as

$$T_2 = \frac{\ell_n 2}{-\varsigma\omega_n} \tag{7}$$

where ζ is the damping ratio and ω_n is the natural frequency. Note that $-\zeta\omega_n$ is the real part of the eigenvalues. If it is positive, the system is unstable and T_2 is also positive, representing the time to double the amplitude. On the other hand, if it is negative, the system is stable and T_2 is negative, representing the time to halve the amplitude. In this latter case, T_2 is replaced by $T_{1/2}$ and 2 in Eq. (7) is replaced by half. For simplicity in the computer output, T_2 will be used in all cases, with the understanding that if it is negative, it should be the time to halve the amplitude.

As can be seen from the preceding considerations, the first step in evaluating the flying qualities is to determine the eigenvalues of an airplane along the flight trajectory. In the present approach, we will numerically integrate the 6-DOF dynamic equations of motion and determine the eigenmodes of motion at the same time at every instant. The matrix for the eigenvalues consists of the first derivatives evaluated at the instant under consideration, not about the trim points as done conventionally. Note that in abnormal flight conditions, there may not be trim points.

It is easier to extract the stability characteristics by formulating the equations in the stability axes. Therefore, the general equations of motion in the following are integrated:

$$\frac{d\alpha}{dt} = f_1 = \left\{\left[\left(-\frac{X}{m} + g\sin\theta\right)\Big/ V - r\sin\beta\right]\sin\alpha + \left[\left(\frac{Z}{m} + g\cos\theta\cos\phi\right)\Big/ V - p\sin\beta\right]\cos\alpha\right\}\Big/\cos\beta + q \tag{8}$$

$$\frac{d\beta}{dt} = f_2 = \left[-\left(\frac{X}{m} - g\sin\theta\right)\sin\beta/V - r\right]\cos\alpha + \left(\frac{Y}{m} + g\cos\theta\sin\phi\right) \times \cos\beta/V\left[-\left(\frac{Z}{m} + g\cos\theta\cos\phi\right)\sin\beta/V + p\right]\sin\alpha \tag{9}$$

$$\frac{dp}{dt} = f_3 = \left[L + \frac{I_{xz}N}{I_{zz}} + I_{xz}\left(1 + \frac{I_{xx} - I_{yy}}{I_{zz}}\right)pq + \left(I_{yy} - I_{zz} - \frac{I_{xz}^2}{I_{zz}}\right)qr\right]\Big/ AI_{xx} \tag{10}$$

$$\frac{dq}{dt} = f_4 = [M + I_{xz}(r^2 - p^2) + (I_{zz} - I_{xx})rp]/I_{yy} \tag{11}$$

$$\frac{dr}{dt} = f_5 = \left[\frac{I_{xz}L}{I_{xx}} + N + \left(I_{xx} - I_{yy} + \frac{I_{xz}^2}{I_{xx}}\right)pq + \left(\frac{I_{yy} - I_{zz}}{I_{xx}} - 1\right)I_{xz}qr\right]\Big/ AI_{zz} \tag{12}$$

$$\frac{d\theta}{dt} = f_6 = q\cos\phi - r\sin\phi \tag{13}$$

$$\frac{d\phi}{dt} = f_7 = p + \tan\theta(q\sin\phi + r\cos\phi) \tag{14}$$

$$\frac{dV}{dt} = f_8 = \left(\frac{X}{m} - g\sin\theta\right)\cos\alpha\cos\beta + \left(\frac{Y}{m} + g\cos\theta\sin\phi\right)\sin\beta + \left(\frac{Z}{m} + g\cos\theta\cos\phi\right)\sin\alpha\cos\beta \tag{15}$$

where $A = 1 - (I_{xz}^2/I_{xx}I_{zz})$, and X, Y, Z, L, M, N are the forces and moments acting on the transport and are estimated from the fuzzy-logic aerodynamic models.

To determine the flying qualities, we need the eigenvalues of the linearized equations. Instead of using an average linearized system, linearization is done at every time instant (i.e., the so-called time linearization, as indicated earlier). In other words, a system of matrix A consisting of $\partial f_i/\partial x_j$ ($i = 1, \ldots, 8$ and $j = 1, \ldots, 8$) is determined while the time integration of the dynamic equation is performed, where x_j stands for α, β, p, q, r, θ, ϕ, and V, for $j = 1, \ldots, 8$. Note that the inertial effects from the moments of inertia are incorporated. The inertial effects could become essential in recovering a flight vehicle from stall or when the conventional control surfaces are not effective. To determine the eigenvalues of A, Francis's QR transformation technique is employed. Unfortunately, it is difficult to identify the individual modes of motion from these eigenvalues from one instant to another because of the rapid changes of aerodynamic forces and moments in turbulence. One approach to solve this problem is to use the approximate modes of motion obtained from decoupled longitudinal and lateral-directional equations as guidance. About the thrust effects, it is known that atmospheric turbulence affects the engine performance through its effects on static and dynamic distortions at the engine face. How to determine its effects is beyond the scope of this paper. In addition, it is inadequate to consider only the local momentum reaction effect at the engine inlet in estimating the thrust effect on stability derivatives, as being done in most textbooks. The overall effect produced, including the exhaust, must be considered as well. Previous study seemed to indicate that the overall effects of power on stability derivatives were mostly not significant. Therefore, although the thrust effects are included, their derivatives are not in the following results.

The decoupled linearized longitudinal equations of motion, which are decoupled from the lateral-directional motions in [10], are given by

$$\dot{u} = -g\theta\cos\theta_1 + X_u u + X_\alpha\alpha + X_{\delta e}\delta e \tag{16}$$

$$U_1\dot{\alpha} - U_1\dot{\theta} = -g\theta\sin\theta_1 + Z_u u + Z_\alpha\alpha + Z_{\dot{\alpha}}\dot{\alpha} + Z_q\dot{\theta} + Z_{\delta e}\delta e \tag{17}$$

$$\ddot{\theta} = M_u u + M_\alpha\alpha + M_{\dot{\alpha}}\dot{\alpha} + M_q\dot{\theta} + M_{\delta e}\delta e \tag{18}$$

where X_u, X_α, and $X_{\delta e}$ are the dimensional variations of force along the X axis with the speed, angle of attack, and elevator angle, respectively; the other dimensional derivatives of Z and M are described and given in [10]. The decoupled lateral-directional equations of motion are

$$U_1\dot{\beta} + U_1\dot{\psi} = g\phi\cos\theta_1 + Y_\beta\beta + Y_p\dot{\phi} + Y_r\dot{\psi} + Y_{\delta a}\delta a + Y_{\delta r}\delta r \tag{19}$$

$$\ddot{\phi} - \bar{A}_1\ddot{\psi} = L_\beta\beta + L_p\dot{\phi} + L_r\dot{\psi} + L_{\delta a}\delta a + L_{\delta r}\delta r \tag{20}$$

$$\ddot{\psi} - \bar{B}_1\ddot{\phi} = N_\beta\beta + N_p\dot{\phi} + N_r\dot{\psi} + N_{\delta a}\delta a + N_{\delta r}\delta r \tag{21}$$

where $\bar{A}_1 = I_{xz}/I_{xx}$ and $\bar{B}_1 = I_{xz}/I_{zz}$; the dimensional derivatives of Y, L, and N are described and given in [10]. The characteristic equations for Eqs. (16–21) are polynomials of the fourth degree and their roots are solved with a quadratic factoring method based on the Lin–Bairstow algorithm in [12].

III. Results and Discussions

A. Aerodynamic Environment

A twin-jet transport encountered severe atmospheric turbulence in revenue flight around an altitude of 10,050 m. Several passengers and crew members sustained injuries in this accident. The present study is to evaluate the dynamic stability characteristics and flying qualities in turbulence response. The aerodynamic environment will first be examined subsequently.

Figure 1 presents the time history of normal acceleration a_n, flight altitude h, angle of attack α, and Mach number M based on QAR. The variations of normal acceleration is shown in Fig. 1a; the highest normal acceleration a_n being 1.75 g at around $t = 3930$ s and the lowest being 0.02 g at around $t = 3932$ s Fig. 1b shows that α is approximately in phase with a_n. When a_n is highest positively (around $t = 3930$ s), the flight altitude is the lowest, as shown in Fig. 1c; the largest α is about 6.5 deg in Fig. 1b, and M is around 0.77 in Fig. 1d. Because α reaches a value of about 6.5 deg in transonic flight, compressibility effect involving shock waves should be important. Note that the turbulent vertical wind field was not measured or estimated in the QAR but is included in the total α.

B. Analysis of Data Predictions

In the present study, the accuracy of the established thrust and aerodynamic models through the fuzzy-logic algorithm is estimated by the sum of squared errors and the square of multiple correlation coefficients (R^2). These measured data must be checked and adjusted to satisfy the kinematic equations through the compatibility analysis [7,8].

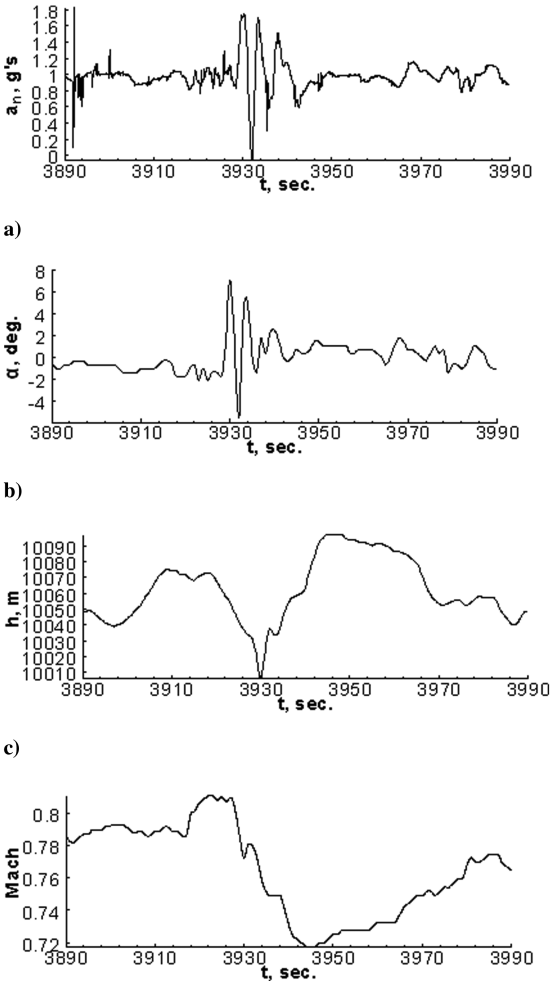

Fig. 1 Time history of flight variables for a twin-jet transport in atmospheric turbulence at the altitude around 10,050 m.

The biggest problem to set up the thrust model is that the climb angles or descent angles may not be accurate. As a result, in plunging motion when EPR is less than 1.0 but the fuel flow rate is still significant, thrust may be predicted to be negative by the thrust model. In this case, thrust is set to zero.

After combining all thrust data in the form of Eq. (1), fuzzy-logic modeling is applied. This is when the robustness in fuzzy-logic modeling is the most useful. Those data points with predicted negative thrust are removed as being not compatible with the cruise thrust model. When the predicted thrust at those zero-thrust data points are positive, these positive thrust values are then used in their places. The second round of filtering is to remove those data points with large differences between the predicted and data values. The filtering applies only to those climbing and descending data points.

Applying this thrust model to the data of the present study case shows no negative thrust even at EPR = 0.740 during severe turbulence encounter, as shown in Fig. 2. The variations of predicted thrust-to-weight ratio T/W, as shown in Fig. 2a, are compatible with those of altitude h in Fig. 1c and fuel flow rate $\dot{m}_f$ in Fig. 2c.

All the required static and dynamic stability derivatives are generated by the aerodynamic coefficients of forces and moments. Figure 3 presents the aerodynamic coefficients of normal force C_z, pitching moment C_m, rolling moment C_l, and yawing moment C_n predicted by the final models. The predicted data by the final models have good agreement with the flight data. The C_m-data scattering in Fig. 3b is most likely caused by turbulence-induced buffeting on the structure, particularly on the horizontal tail.

C. Analysis of Pilot's Responses in Operations

Before presenting the eigenvalues, the key flight variables are presented in Fig. 4 to show the pilot's possible response in operations. In Fig. 4a, both α and β are the total values, including the turbulence effects. It is shown that α exceeds 6.5 deg and reaches -5.5 deg at transonic speeds. Both the pitch angle θ and roll angle ϕ vary similarly, particularly the latter, as shown in Fig. 4b. The pitch angle does not vary as much as the angle of attack. The yaw rate is not shown because it is small throughout. Note that the pitch and roll

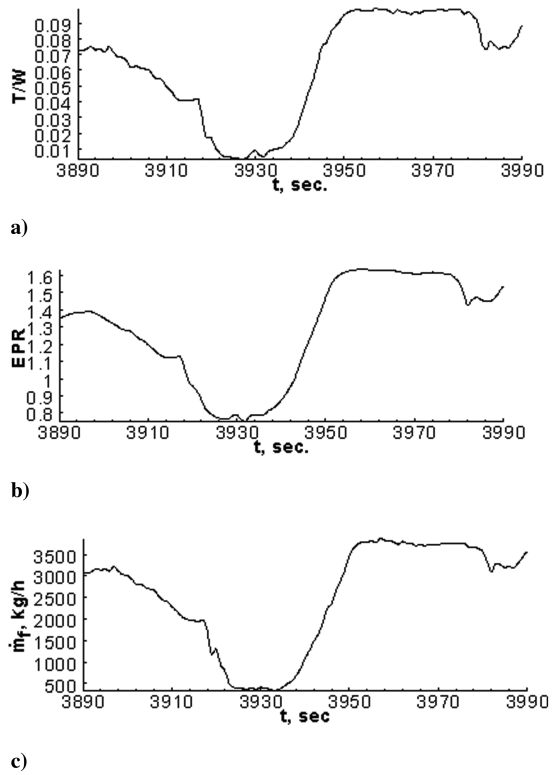

Fig. 2 Predicted thrust-to-weight ratio with the associated thrust variables for a twin-jet transport encountering severe atmospheric turbulence at cruise altitudes around 10,050 m.

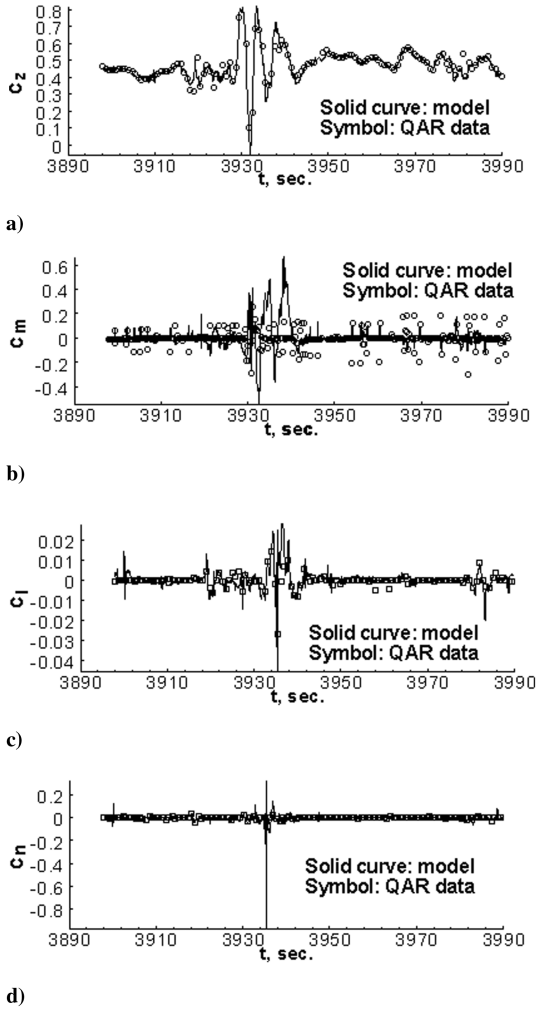

Fig. 3 Predicted aerodynamic coefficients in normal force and moments for a twin-jet transport encountering severe atmospheric turbulence at cruise altitudes around 10,050 m.

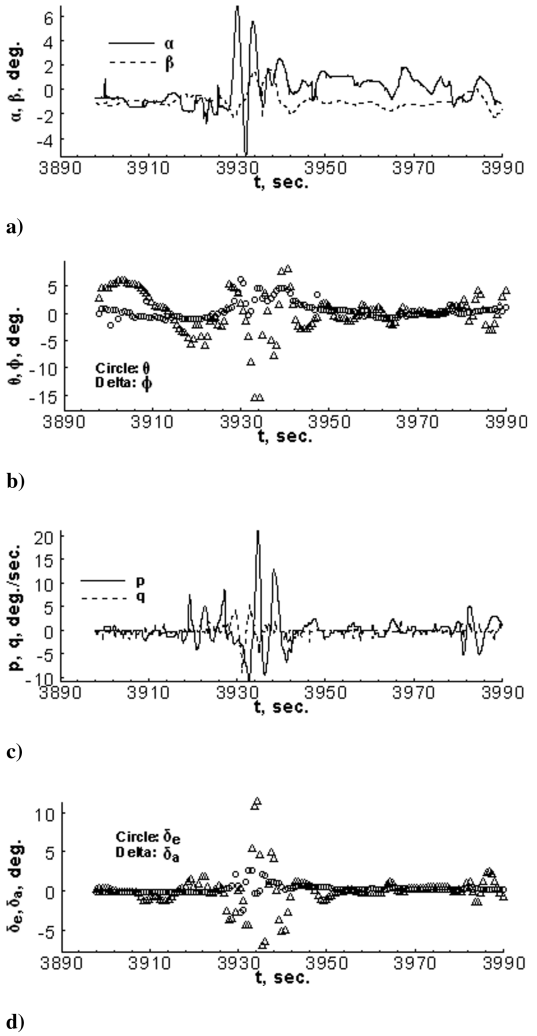

Fig. 4 Flight and control variables for a twin-jet transport encountering severe atmospheric turbulence at high altitudes and high Mach number.

angles usually represent the cues to a pilot in making the control decision when the autopilot is deactivated. Both the pitch and roll rates are also significant in Fig. 4c. In normal flight, both typically should be small, particularly at transonic speeds. It is shown that there are considerable control surface activities in Fig. 4d, even though pilots are usually instructed in training to not manually control the airplane in severe turbulence, unless the autopilot is automatically deactivated. For the twin-jet transport under study, the QAR indicated the autopilot disengagement from $t = 3929$ to 3938 s for 9 s.

The characteristic modes in flight dynamics depend on not only mass and moments of inertia, but also the aerodynamic derivatives and thrust derivatives. In the present analysis, the required derivatives are all estimated with a central-difference scheme by using the established aerodynamics models. Here, the thrust derivatives are not included, because of the uncertainty in the turbulence effects on thrust. Some main aerodynamic derivatives along the flight path are presented in Fig. 5. Note that these derivatives are evaluated at the instantaneous conditions, instead of about the trim conditions as indicated earlier. Because the autopilot is automatically deactivated at $t = 3929$ s and the highest a_n is 1.75 g at around $t = 3930$ s and the lowest is 0.02 g at around $t = 3932$ s, the evaluations of stability characteristics between the time segments of 3927–3933 s are emphasized in the present paper. From the point of view of static stability, the configuration initially has longitudinal stability ($C_{m\alpha} < 0$) in Fig. 5a, stable longitudinal damping ($C_{mq} < 0$) in Fig. 5b, lateral stability ($C_{l\beta} < 0$) in Fig. 5c, directional stability ($C_{n\beta} > 0$) in Fig. 5c, small roll damping ($C_{lp} < 0$) in Fig. 5d, and insufficient directional damping (C_{nr} small or positive) in Fig. 5d.

During the plunging motion, in the period of $t = 3928.5$–3930.5 s, the static stability tends to get worse. Note that in Fig. 5b, the oscillatory derivatives are defined as

$$(C_{mq})_{\text{osc}} = C_{mq} + C_{m\dot{\alpha}} \tag{22}$$

$$(C_{zq})_{\text{osc}} = C_{zq} + C_{z\dot{\alpha}} \tag{23}$$

In Fig. 5d, the oscillatory derivatives [13] are defined as

$$(C_{lp})_{\text{osc}} = C_{lp} + C_{l\dot{\beta}} \sin\alpha \tag{24}$$

$$(C_{nr})_{\text{osc}} = C_{nr} - C_{n\dot{\beta}} \cos\alpha \tag{25}$$

For the present configuration, the dynamic derivatives (i.e., $\dot{\alpha}$ and $\dot{\beta}$ derivatives) tend to be small. However, the $\dot{\alpha}$ derivative is to improve the stability in pitch, and the $\dot{\beta}$ derivative is to make the directional stability more unstable [i.e., $(C_{nr})_{\text{osc}}$ more positive]. These results indicate that the turbulent crosswind has a significant effect on directional stability and damping. The effects of the $\dot{\alpha}$ derivative on C_{zq} and the $\dot{\beta}$ derivative on C_{lp} are small and therefore are not plotted. To be stable, $(C_{zq})_{\text{osc}} < 0$, $(C_{mq})_{\text{osc}} < 0$, $(C_{lp})_{\text{osc}} < 0$, and $(C_{nr})_{\text{osc}} < 0$. Physically, if it is unstable, the motion will be divergent in oscillatory motions. In calculating the eigenmodes, these oscillatory derivatives are those used in forming the characteristic equations.

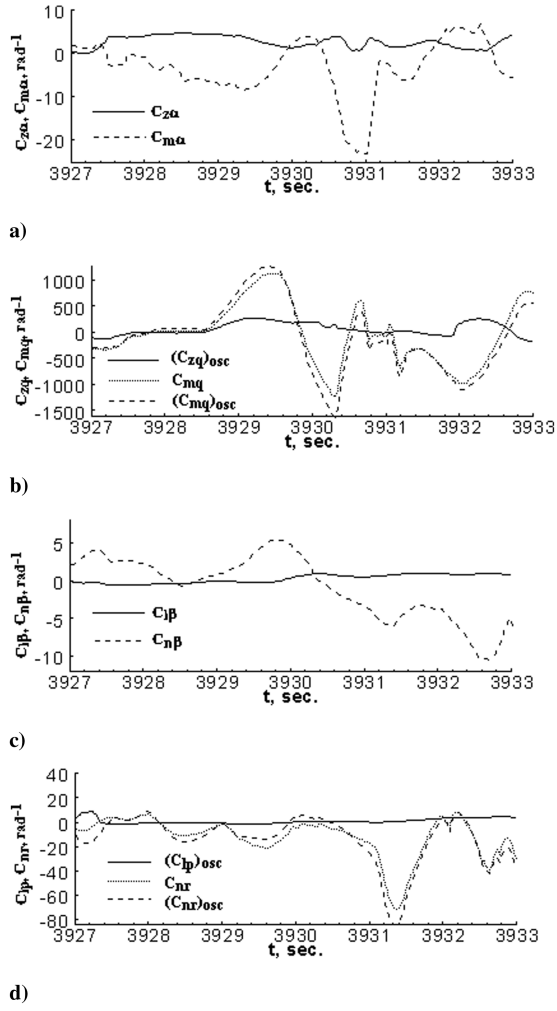

Fig. 5 Variation of main longitudinal and lateral-directional aerodynamic derivatives along the flight path.

D. Analysis of Flying Qualities

To evaluate the dynamic stability, we need the eigenvalues of the characteristic equations, the formulation of which was mentioned earlier [see the paragraph after Eq. (15)]. The present formulation is truly a coupled 6-DOF formulation, because the lateral-directional equations of motion include not only longitudinal variables, such as θ, but some mixed derivatives, such as C_{mp}, are included as well. The results for the short-period mode are compared with the decoupled formulation in Fig. 6. The eigenvalues are expressed as

$$\lambda = \lambda_r + i\lambda_i \tag{26}$$

Figure 6 shows that the short-period mode is stable initially (λ_r being negative) but becomes small in damping later. In general, the agreement between the present 6-D formulation and that of a decoupled one appears to be good. This implies that the 6-D effects on the short-period mode are small. On the other hand, the phugoid mode (or the plunging mode in the present case) is largely affected by the 6-D effects. In general, the 6-D effects are to make the plunging less unstable, or more stable. In the 6-D formulation, the natural frequency is mostly zero throughout, whereas the 3-D decoupled formulation produces very small, but not zero, frequency.

The lateral-directional eigenvalues are compared in Fig. 7. It is shown that the results from both the 3-D and 6-D formulations agree very well. One notable result is that the so-called Dutch roll mode exhibits frequencies much higher than the short-period mode (Fig. 6) and hence could very well be mistaken as the short-period mode without the guidance from the 3-D formulation. The high-frequency oscillation represents rolling and yawing motions with relatively low amplitudes but higher frequencies. There are larger discrepancies

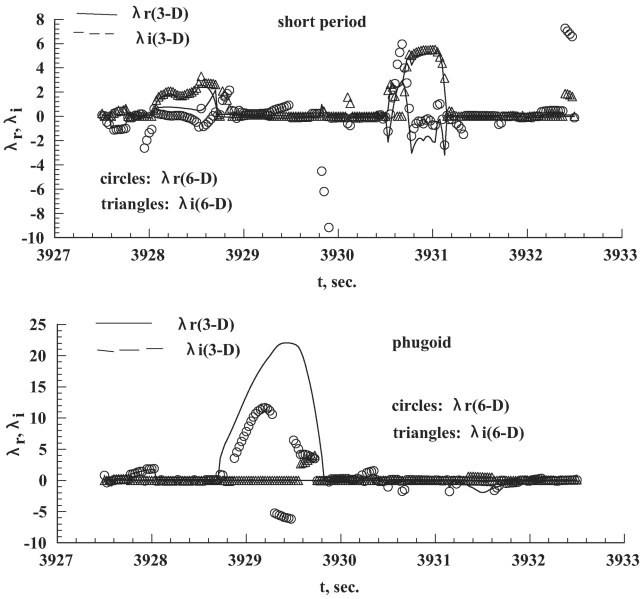

Fig. 6 Comparison of eigenvalues of longitudinal modes of motion for a twin-jet transport in encountering severe atmospheric turbulence.

between the 3-D and 6-D formulations in the roll mode at some points. The roll mode is mostly stable, except at points corresponding to those points with high roll rates (Fig. 4c).

The flying quality for the phugoid mode can be examined through the time to double (T_2) or to halve ($T_{1/2}$) the amplitude. In the present study, we will focus on the plunging (i.e., phugoid) mode with the corresponding eigenvalues presented in Fig. 8. Only the 6-D results are presented. In the military specifications, T_2 must be greater than 55 s for the phugoid mode in level III in the military specifications. The flying qualities in civil airplane design have no such numerical guidelines. They are indicated here for reference only. The real part of the eigenvalues in Eq. (7) is defined as λ_r, and so T_2 can be rewritten as

$$T_2 = \ell_n(2)/\lambda_r \tag{27}$$

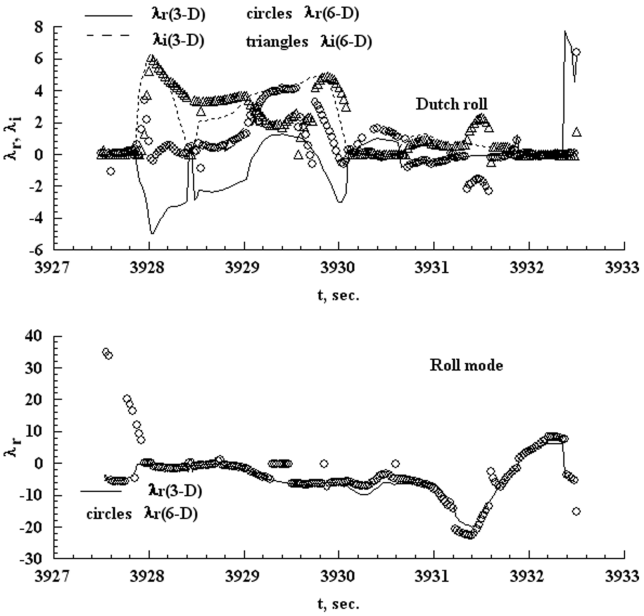

Fig. 7 Comparison of eigenvalues of lateral-directional modes of motion for a twin-jet transport in encountering severe atmospheric turbulence.

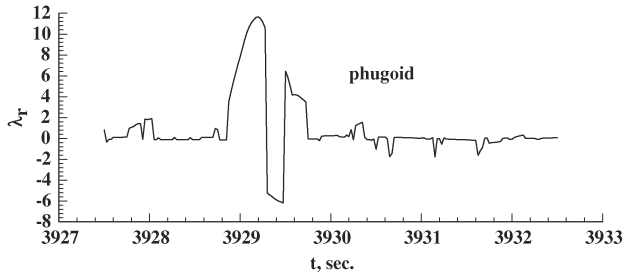

Fig. 8 Flying qualities parameters of the plunging (or phugoid) mode for a twin-jet transport in encountering severe atmospheric turbulence.

Figure 8 shows large positive λ_r in the plunging mode when the airplane is moving downward. It follows that T_2 is very small (very unstable).

It is of interest to examine the control power to determine if the motion is related to control activities. The dimensional control powers are presented in Fig. 9. They are defined as

$$Z_{\delta e} = \frac{\bar{q}SC_{z\delta e}}{mV} \tag{28}$$

$$M_{\delta e} = \frac{\bar{q}S\bar{c}C_{m\delta e}}{I_{yy}} \tag{29}$$

The definition of Eq. (28) is slightly different from that in Eq. (17) in that there is V in the denominator in Eq. (28) but not in Eq. (17). Note that $C_{z\delta e}$ is positive pointing downward (in the positive z direction) but should be negative in the normal situation. The loss of damping tends to coincide with the motion of plunging downward, as shown in Figs. 8 and 9c. It is shown that during the period of fast altitude variation, $t = 3929$–3930.8 s in Fig. 9c, the available control is ineffective in Figs. 9a and 9b ($M_{\delta e} < 0.0$ and $Z_{\delta e} < 0.0$ to be effective). It is called *ineffective* instead of control reversal, because the motion is not caused by the control input. Although there are considerable control deflections around the time of high gravity

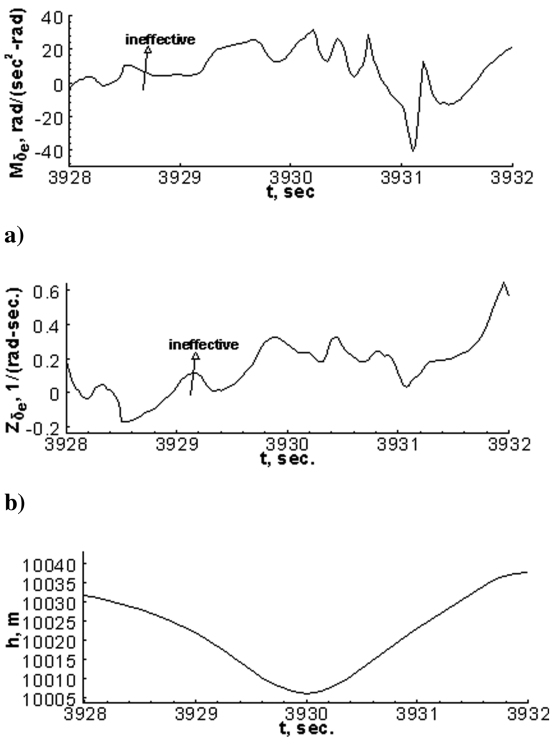

Fig. 9 Variation of dimensional longitudinal control powers for a twin-jet transport in severe turbulence.

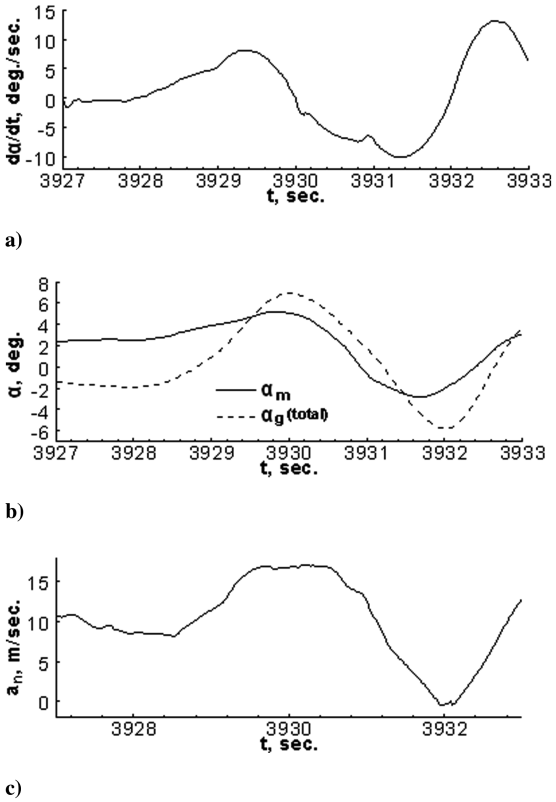

Fig. 10 Flight environments in plunging mode to determine the hazard index.

load (Fig. 4d) and there is no control effectiveness before $t = 3931$, it may be concluded that the high pitch angle in Fig. 4b must be caused by the turbulence-induced motion. Conventionally, the elevator is designed to change the angle of attack to achieve the desirable control. At a transonic speed, this may not be desirable, as shock-induced separation may occur if α is increased from the trim value. In addition, it takes time to increase the angle of attack to produce more lift because of large moments of inertia I_{yy}. The conclusion about the control surface deflections is that they are most likely caused by turbulence-induced buffeting.

Figure 10a presents the time history of dynamic derivatives ($\dot{\alpha}$ derivative), where $\dot{\alpha}$ is $d\alpha_g/dt$. In Fig. 10b, α_m and α_g represent angles of attack due to motion and the total angle of attack, respectively. The difference between the two, $\Delta\alpha = \alpha_g - \alpha_m$, represents the angle of attack from the turbulence. In Fig. 10c, it is shown that the peak gravity load in the present case is mainly caused by the aircraft motion. The fast altitude drop is initiated by the downwind. Moving downward increases the angle of attack due to motion. Comparing Fig. 8 with Fig. 10c, the maximum gravity load does not coincide with the maximum loss of damping. On the other hand, the atmospheric turbulence that causes safety concerns is one that involves sudden plunging motions and may not coincide with the peak load in time. Therefore, if the maximum gravity load, or the minimum value of the gravity load, is used as the hazard index, it will not be possible to correlate the severity of plunging motion. Therefore, the value of damping (i.e., λ_r) is perhaps the most suitable parameter. When it is large positive, the amount of altitude change is expected to be large as well. Note that the maximum value of positive λ_r tends to coincide with large positive $d\alpha_g/dt$ ($\dot{\alpha}$) when α_m is positive (i.e., moving downward) in Fig. 10a. In a way, the effect of $d\alpha_g/dt$ can be viewed as that due to vertical windshear.

IV. Conclusions

The main objective in this paper was to evaluate the dynamic stability characteristics and to demonstrate the flying qualities on a twin-jet transport in severe atmospheric turbulence with sudden

plunging motion in transonic flight. Unsteady aerodynamic models and a thrust model were developed for the purpose of analyzing the aircraft response. The twin-jet transport under study was shown to have static instability and unstable damping in the plunging motion. The results also indicated that the turbulent crosswind had significant effect on directional stability and damping. The dynamic stability and flying qualities were examined through digital simulation. The plunging mode was shown to be very unstable (i.e., large positive real part of the eigenvalues) when the airplane was moving downward. The magnitude of the real part of eigenvalues could be related to the severity of plunging motion. It was shown that the high gravity load was mainly caused by the aircraft motion.

Acknowledgments

This research project is sponsored by grant NSC97-3114-P-707-001-Y from the National Science Council (NSC). The accomplishment in this project is part of the requirements set by the Aviation Safety Council (ASC) of the Executive Yuan.

References

[1] Hamilton, D. W., and Proctor, F. H., "An Aircraft Encounter with Turbulence in the Vicinity of a Thunderstorm," AIAA Paper 2003-4075, 2003.

[2] Cornman, L. B., Morse, C., and Cunning, G., "Real-Time Estimation of Atmospheric Turbulence Severity from In-Situ Aircraft Measurements," *Journal of Aircraft*, Vol. 32, No. 1, 1995, pp. 171–177. doi:10.2514/3.46697

[3] Stewart, E. C., "Description of a Normal-Force In-Situ Turbulence Algorithm for Airplanes," NASA TM-2003-212666, Dec. 2003.

[4] Buck, W. K., Bowles, R. L., and Newman, B. A., "Aircraft Acceleration Prediction due to Atmospheric Disturbances with Flight Data Validation," AIAA Paper 2004-4826, 2004.

[5] Lee, Y. N., and Lan, C. E., "Analysis of Random Gust Response with Nonlinear Unsteady Aerodynamics," *AIAA Journal*, Vol. 38, No. 8, Aug. 2000, pp. 1305–1312. doi:10.2514/2.1113

[6] Li, J., and Lan, C. E., "Unsteady Aerodynamic Modeling of Aircraft Response to Atmospheric Turbulence," AIAA Paper 2003-5473, Aug. 2003.

[7] Pan, C., and Lan, C. E., "Estimation of Aerodynamic Characteristics of a Jet Transport Using Accident FDR Data," AIAA Paper 2002-4494, Aug. 2002.

[8] Weng, C. T., Ho. C. S., Lan, C. E., and Guan, M., "Aerodynamic Analysis of a Jet Transport in Windshear Encounter During Landing," *Journal of Aircraft*, Vol. 43, No. 2, Mar.–Apr. 2006, pp. 419–427. doi:10.2514/1.15605

[9] Roskam, J., *Airplane Design*, Pt. 5, DAR Corp., Lawrence, KS, pp. 197–206.

[10] Roskam, J., *Airplane Flight Dynamics and Automatic Flight Controls*, Pt. I, DAR Corp., Lawrence, KS, 2003.

[11] "Flying Qualities of Piloted Airplanes," U.S. Dept. of Defense, MIL-SPEC MIL-F-8785C, Nov. 1980.

[12] Hovanessian, S. A., and Pipes, L. A., *Digital Computer Methods in Engineering*, McGraw–Hill, New York, 1969.

[13] Lan, C. E., Bianchi, Silvia, and Brandon, Jay, M., "Estimation of Nonlinear Aerodynamic Roll Models for Identification of Uncommanded Rolling Motions," *Journal of Aircraft*, Vol. 45, No. 3, May–June 2008, pp. 916–922. doi:10.2514/1.30388